der(9)-forward, 5′-GGAAAGGAATGGAATGAAATCAACGCG-3′; der(9)-reverse, 5′-CCAGGACAGCGTCTCACTCTCCATA-3′ (495-bp). Junction fragments were amplified by PCR using these primer-sets on DNAs of the patient and her parents.

RESULTS

G-banded chromosomal analysis revealed a balanced translocation t(1;9)(q32;q13). Her parents showed a normal karyotype (data not shown), indicating that the translocation occurred de novo. Subsequent FISH analysis demonstrated that the breakpoint in chromosome 1 was covered by the clones, RP11-1109h22 and 134f21, showing signals all on normal chromosome 1 and derivatives chromosomes 1 and 9 (Fig. 2A,B). The overlapping region of these two clones was localized within the *SRGAP2* locus (Fig. 2A). The 5′-part of *SRGAP2* transcript was not mapped in the Human Genome browser (both in NCBI Build 36.1/hg18 and GRCh37/hg19 assembly) because the genomic contigs covering the immediately upstream regions of *SRGAP2* gene were absent. Thus, we described the putative exon number based on the order of mappable exons to the existing genomic database. The breakpoint was further narrowed down by FISH analysis using long PCR products as probes (Fig. 2A). Probe II showed weak but clear signals all in on chromosome 1, and derivative chromosomes 1 and 9, suggesting that the breakpoint was located within probe II (data not shown). It was of note that the probe II is associated with a segmental duplication (Fig. 2A). Southern hybridization analysis using probes P1 and P3 detected different aberrant bands only in the patient (Fig. 2A,C), indicating that the 1q32 breakpoint was located at the region between the two probes. P2 did not show any aberrant bands in Southern analysis, suggesting that a small deletion may have occurred near the breakpoint (Fig. 2A,C). Inverse PCR [Triglia et al., 1988] on *Eco*RI- and *Pst*I-digested DNA was successful in obtaining der(1) and der(9) breakpoint-junction fragments, respectively. Sequence analysis showed that the 1q32 translocation breakpoint was located within the putative intron 5 of *SRGAP2*, and exon 5 was completely deleted (Fig. 2A). Sequences of the 9q13 breakpoint were not uniquely mapped to reference sequences. However, sequences of 3′-end of the der(1) junction fragment (approximately 6.1-kb apart from the breakpoint) were similar to satellite 3 sequences (GeneBank accession number AF035810.1) (Fig. 2E), suggesting that 9q13 breakpoint was located in the heterochromatin region. Breakpoint-specific PCR analysis of the patient and her parents confirmed that the rearrangements occurred de novo (Fig. 2F). To check genomic copy number alterations accompanied by the rearrangement, GeneChip Human Mapping 250K *Nsp*I (Affymetrix, Santa Clara, CA) was performed. Besides two known copy number variations, no other imbalances were detected (data not shown).

DISCUSSION

SRGAP2 is a member of Slit-Robo Rho GTPase activating proteins with three domains: an N-terminal F-BAR domain, a RhoGAP domain, and an SH3 domain [Wong et al., 2001; Guerrier et al., 2009]. There are three variants of *SRGAP2* transcripts in humans: variant 1 (GenBank accession number NM_015326.2), variant 2 (GenBank accession number NM_001042758.1), and variant 3 (GenBank accession number NM_001170637.1). In all three variants, the coding proteins commonly possess F-BAR, RhoGAP, and SH3 domains except for an amino acid deletion in F-BAR domain in variant 2. Mouse *Srgap2* is expressed in the entire developing cortex including proliferative zones and postmitotic regions [Bacon et al., 2009; Guerrier et al., 2009]. It has been reported that the SRGAP2 protein negatively regulates neuronal migration and induce neurite outgrowth and branching through its F-BAR domain [Guerrier et al., 2009]. In addition, GAP activity of the SRGAP2 protein specifically downregulate Rac1 [Guerrier et al., 2009]. Mutations in *ARHGEF6*, Rac1/Cdc42 specific GEF, cause X-linked mental retardation [Kutsche et al., 2000]. Moreover, mutation and/or disruption of *OPHN1* and *SRGAP3*, both encoding Rac1-GAPs, are associated with severe mental retardation [Billuart et al., 1998; Endris et al., 2002], indicating the importance of Rac1 regulation in human brain development. Thus, SRGAP2 is likely to play important roles in developing brain in humans through the ability of the F-BAR and RhoGAP domains. It would be interesting to analyze

FIG. 2. Genomic characterization of t(1;9)(q32;q13). A: Schematic representation of the reciprocal translocation, t(1;9)(q32;q13) (top). A summarized physical map covering the 1q32.1 translocation breakpoint is indicated (middle). RP11-1109h22 and 134f21, and PCR probe II span the translocation breakpoint (longitudinal dashed line) in association with the segmental duplication. Four RefSeq genes, including *SRGAP2* spanning the breakpoint, are presented. Note that absence of genomic contigs of the immediately upstream region of the *SRGAP2* gene. More detailed maps are shown (bottom). A partial restriction map (E, *Eco*RI; P, *Pst*I), probes for southern hybridization (P1–P3), and putative exons 5–7 of *SRGAP2* are indicated. Translocation breakpoint (longitudinal dashed line) accompanied with a 1,575-bp deletion encompassing exon 5 of *SRGAP2* (red thick dashed line) are located between P1 and P3. B: FISH analysis using RP11-1109h22 as a probe showed clear signals on chromosome 1, and der(1) (white arrowheads) and der(9) chromosomes (white arrow). Cross-hybridization was also observed to segmental duplications located at pericentric regions of chromosome 1 and derivative chromosome 1. C: Southern hybridization using probes P1, P2, and P3 on genomic DNAs of the patient and her parents. Arrow shows aberrant bands specific to the patient (not observed in parental DNA). Pt, patient; Fa, father; Mo, mother. D: Breakpoint junction sequences of der(1) and der(9). In upper part, top and bottom sequence strands show chromosome 1 and derivative chromosome 1 sequences, respectively. In lower part, top and bottom strands show derivative chromosome 9 and normal chromosome 1 sequences, respectively. Breakpoint positions are marked with small longitudinal lines based on the UCSC genome browser coordinate (version Mar. 2006). Asterisks indicate nucleotides identical to normal chromosomes. E: Sequences of the 3′-end of the der(1) junction fragment. Top and bottom sequence strands show der(1) and satellite 3 sequences, respectively, showing homology between two sequences. F: Breakpoint-specific PCR analysis of the patient's family. Primers specific to der(1) and der(9) breakpoints could successfully amplify 1,098- and 495-bp products, respectively, only from the patient (Pt), indicating the translocation occurred de novo. M, size marker; Fa, father; Mo, mother.

SRGAP2 in a large cohort of patients presenting with early epileptic encephalopathy including West syndrome. Although full-length *SRGAP2* transcripts (functional), which include sequences of putative exons 1–20 at 1q32.1, have been deposited in GeneBank, 5′-part of the *SRGAP2* transcript is not mapped in the Human Genome browser. Furthermore, seven exons of *SRGAP2* were again mapped to two separated segmental duplications at 1q21.1 and 1p11.2 with sequence similarities of 99.29% and 99.30%, respectively (Fig. 2A). This complex genomic structure interfered with full-blown mutation screening especially for the 1,356-bp coding region including the F-BAR domain. A microdeletion within two separate segmental duplications in *SRGAP2* locus has been found in 2 out of 90 Yoruban individuals (presumably with normal phenotype) from the HapMap Project using custom high-density oligonucleotide arrays [Matsuzaki et al., 2009]. However, it is uncertain whether they could confirm the precise locations of the deletions by another method. Thus, there remains a possibility that the deletion actually ocurred at highly homologous genomic segments located at 1q21.1 and 1p11.2. Further descriptions about aberrations of the *SRGAP2* gene will be required for establishing in a causative role in early infantile epileptic encephalopathy.

The 9q13 breakpoint is likely to reside within the heterochromatic region. It is possible that some genes adjacent to 1q32.1 breakpoint would suffer from gene silencing by the position effect. *IKBKE* is an IKK (inhibitor of nuclear factor kappaB kinase)-related kinase that is essential for interferon-inducible antiviral transcriptional response [Tenoever et al., 2007]. *Ikbke* knockout mice are protected from high-fat diet-induced obesity, chronic inflammation in liver and fat, hepatic steatosis, and whole-body insulin resistance [Chiang et al., 2009]. However, neurological abnormalities have never been reported. *RASSF5* is a member of the Ras association domain family. A crutial role in the integrin-mediated adhesion and migration of lymphocytes and dendritic cells has been shown in *Rassf5*-deficient mice, but neurological abnormalities have never been mentioned [Katagiri et al., 2004]. Thus, *IKBKE* and *RASSF5*, two adjacent genes to *SRGAP2*, are less likely to be involved in infantile epileptic encephalopathy.

In conclusion, we described a patient with early infantile epilepsitic encephalopathy, carrying a de novo reciprocal translocation disrupting the *SRGAP2* gene. Clonic convulsions and atypical suppression-burst patterns on EEG at early infantile period did not fit into either OS or EME. However, the seizures became brief tonic spasms, and hypsarrhythmia on EEG was noticed, indicating transition to West syndrome. Disruption of *SRGAP2* may be related to West syndrome which has heterogeneous backgrounds [Kato, 2006].

ACKNOWLEDGMENTS

We would like to thank the patient and her families for their participation in this study. This work was supported by Research Grants from the Ministry of Health, Labour and Welfare (H.S. and N. Matsumoto), Grant-in-Aid for Scientific Research from Japan Society for the Promotion of Science (N. Matsumoto), Grant-in-Aid for Young Scientist from Japan Society for the Promotion of Science (H.S.), Research Promotion Fund from Yokohama Foundation for Advancement of Medical Science (H.S.), Research Grants from the Japan Epilepsy Research Foundation (H.S.), and Research Grant from Naito Foundation (N. Matsumoto).

REFERENCES

Bacon C, Endris V, Rappold G. 2009. Dynamic expression of the Slit-Robo GTPase activating protein genes during development of the murine nervous system. J Comp Neurol 513:224–236.

Billuart P, Bienvenu T, Ronce N, des Portes V, Vinet MC, Zemni R, Roest Crollius H, Carrie A, Fauchereau F, Cherry M, Briault S, Hamel B, Fryns JP, Beldjord C, Kahn A, Moraine C, Chelly J. 1998. Oligophrenin-1 encodes a rhoGAP protein involved in X-linked mental retardation. Nature 392:923–926.

Brose K, Bland KS, Wang KH, Arnott D, Henzel W, Goodman CS, Tessier-Lavigne M, Kidd T. 1999. Slit proteins bind Robo receptors and have an evolutionarily conserved role in repulsive axon guidance. Cell 96:795–806.

Chiang SH, Bazuine M, Lumeng CN, Geletka LM, Mowers J, White NM, Ma JT, Zhou J, Qi N, Westcott D, Delproposto JB, Blackwell TS, Yull FE, Saltiel AR. 2009. The protein kinase IKKepsilon regulates energy balance in obese mice. Cell 138:961–975.

Djukic A, Lado FA, Shinnar S, Moshe SL. 2006. Are early myoclonic encephalopathy (EME) and the Ohtahara syndrome (EIEE) independent of each other? Epilepsy Res 70:S68–S76.

Endris V, Wogatzky B, Leimer U, Bartsch D, Zatyka M, Latif F, Maher ER, Tariverdian G, Kirsch S, Karch D, Rappold GA. 2002. The novel Rho-GTPase activating gene MEGAP/ srGAP3 has a putative role in severe mental retardation. Proc Natl Acad Sci USA 99:11754–11759.

Guerrier S, Coutinho-Budd J, Sassa T, Gresset A, Jordan NV, Chen K, Jin WL, Frost A, Polleux F. 2009. The F-BAR domain of srGAP2 induces membrane protrusions required for neuronal migration and morphogenesis. Cell 138:990–1004.

Hall A. 1998. Rho GTPases and the actin cytoskeleton. Science 279: 509–514.

Kalscheuer VM, Tao J, Donnelly A, Hollway G, Schwinger E, Kubart S, Menzel C, Hoeltzenbein M, Tommerup N, Eyre H, Harbord M, Haan E, Sutherland GR, Ropers HH, Gecz J. 2003. Disruption of the serine/ threonine kinase 9 gene causes severe X-linked infantile spasms and mental retardation. Am J Hum Genet 72:1401–1411.

Katagiri K, Ohnishi N, Kabashima K, Iyoda T, Takeda N, Shinkai Y, Inaba K, Kinashi T. 2004. Crucial functions of the Rap1 effector molecule RAPL in lymphocyte and dendritic cell trafficking. Nat Immunol 5:1045–1051.

Kato M. 2006. A new paradigm for West syndrome based on molecular and cell biology. Epilepsy Res 70:S87–S95.

Kato M, Saitoh S, Kamei A, Shiraishi H, Ueda Y, Akasaka M, Tohyama J, Akasaka N, Hayasaka K. 2007. A longer polyalanine expansion mutation in the ARX gene causes early infantile epileptic encephalopathy with suppression-burst pattern (Ohtahara syndrome). Am J Hum Genet 81: 361–366.

Kato M, Saitoh S, Kamei A, Shiraishi H, Ueda Y, Akasaka M, Tohyama J, Akasaka N, Hayasaka K., 2008. Genetic etiology of age-dependent epileptic encephalopathy in infancy: Longer polyalanine expansion in ARX causes earlier onset and more severe phenotype. In: Takahashi T, Fukuyama Y, editors. Biology of seizure susceptibility in developing brain. Montrouge, Paris: John Libbey Eurotext. pp. 75–86.

Kutsche K Yntema H Brandt A Jantke I Nothwang HG Orth U Boavida MG David D Chelly J Fryns JP Moraine C Ropers HH Hamel BC van Bokhoven H Gal A 2000 Mutations in ARHGEF6 encoding a guanine nucleotide exchange factor for Rho GTPases in patients with X-linked mental retardation Nat Genet 26:247–250.

Lamarche N, Hall A. 1994. GAPs for rho-related GTPases. Trends Genet 10:436–440.

Li HS, Chen JH, Wu W, Fagaly T, Zhou L, Yuan W, Dupuis S, Jiang ZH, Nash W, Gick C, Ornitz DM, Wu JY, Rao Y. 1999. Vertebrate slit, a secreted ligand for the transmembrane protein roundabout, is a repellent for olfactory bulb axons. Cell 96:807–818.

Matsuzaki H, Wang PH, Hu J, Rava R, Fu GK. 2009. High resolution discovery and confirmation of copy number variants in 90 Yoruba Nigerians. Genome Biol 10:R125.

Molinari F, Raas-Rothschild A, Rio M, Fiermonte G, Encha-Razavi F, Palmieri L, Palmieri F, Ben-Neriah Z, Kadhom N, Vekemans M, Attie-Bitach T, Munnich A, Rustin P, Colleaux L. 2005. Impaired mitochondrial glutamate transport in autosomal recessive neonatal myoclonic epilepsy. Am J Hum Genet 76:334–339.

Nannya Y, Sanada M, Nakazaki K, Hosoya N, Wang L, Hangaishi A, Kurokawa M, Chiba S, Bailey DK, Kennedy GC, Ogawa S. 2005. A robust algorithm for copy number detection using high-density oligonucleotide single nucleotide polymorphism genotyping arrays. Cancer Res 65: 6071–6079.

Ohtahara S, Yamatogi Y. 2006. Ohtahara syndrome: With special reference to its developmental aspects for differentiating from early myoclonic encephalopathy. Epilepsy Res 70:S58–S67.

Saitsu H, Kato M, Mizuguchi T, Hamada K, Osaka H, Tohyama J, Uruno K, Kumada S, Nishiyama K, Nishimura A, Okada I, Yoshimura Y, Hirai S, Kumada T, Hayasaka K, Fukuda A, Ogata K, Matsumoto N. 2008. De novo mutations in the gene encoding STXBP1 (MUNC18-1) cause early infantile epileptic encephalopathy. Nat Genet 40:782–788.

Stromme P, Mangelsdorf ME, Shaw MA, Lower KM, Lewis SM, Bruyere H, Lutcherath V, Gedeon AK, Wallace RH, Scheffer IE, Turner G, Partington M, Frints SG, Fryns JP, Sutherland GR, Mulley JC, Gecz J. 2002. Mutations in the human ortholog of Aristaless cause X-linked mental retardation and epilepsy. Nat Genet 30:441–445.

Tenoever BR, Ng SL, Chua MA, McWhirter SM, Garcia-Sastre A, Maniatis T. 2007. Multiple functions of the IKK-related kinase IKKepsilon in interferon-mediated antiviral immunity. Science 315:1274–1278.

Triglia T, Peterson MG, Kemp DJ. 1988. A procedure for in vitro amplification of DNA segments that lie outside the boundaries of known sequences. Nucleic Acids Res 16:8186.

Weaving LS, Christodoulou J, Williamson SL, Friend KL, McKenzie OL, Archer H, Evans J, Clarke A, Pelka GJ, Tam PP, Watson C, Lahooti H, Ellaway CJ, Bennetts B, Leonard H, Gecz J. 2004. Mutations of CDKL5 cause a severe neurodevelopmental disorder with infantile spasms and mental retardation. Am J Hum Genet 75:1079–1093.

Wong K, Ren XR, Huang YZ, Xie Y, Liu G, Saito H, Tang H, Wen L, Brady-Kalnay SM, Mei L, Wu JY, Xiong WC, Rao Y. 2001. Signal transduction in neuronal migration: Roles of GTPase activating proteins and the small GTPase Cdc42 in the Slit-Robo pathway. Cell 107:209–221.

Wu W, Wong K, Chen J, Jiang Z, Dupuis S, Wu JY, Rao Y. 1999. Directional guidance of neuronal migration in the olfactory system by the protein Slit. Nature 400:331–336.

Yao Q, Jin W-L, Wang Y, Ju G. 2008. Regulated shuttling of Slit-Robo-GTPase activating proteins between nucleus and cytoplasm during brain development. Cell Mol Neurobiol 28:205–221.

Published in final edited form as:
Am J Med Genet A. 2011 July ; 155(7): 1511–1516. doi:10.1002/ajmg.a.34074.

Spectrum of *MLL2* (*ALR*) mutations in 110 cases of Kabuki syndrome

Mark C. Hannibal[1,2,*], **Kati J. Buckingham**[1,*], **Sarah B. Ng**[3,*], **Jeffrey E. Ming**[4], **Anita E. Beck**[1,2], **Margaret J. McMillin**[2], **Heidi I. Gildersleeve**[1], **Abigail W. Bigham**[1], **Holly K. Tabor**[1,2], **Heather C. Mefford**[1,2], **Joseph Cook**[1], **Koh-ichiro Yoshiura**[5], **Tadashi Matsumoto**[5], **Naomichi Matsumoto**[6], **Noriko Miyake**[6], **Hidefumi Tonoki**[7], **Kenji Naritomi**[8], **Tadashi Kaname**[8], **Toshiro Nagai**[9], **Hirofumi Ohashi**[10], **Kenji Kurosawa**[11], **Jia-Wei Hou**[12], **Tohru Ohta**[13], **Deshung Liang**[14], **Akira Sudo**[15], **Colleen A. Morris**[16], **Siddharth Banka**[17], **Graeme C. Black**[17], **Jill Clayton-Smith**[17], **Deborah A. Nickerson**[3], **Elaine H. Zackai**[4], **Tamim H. Shaikh**[18], **Dian Donnai**[17], **Norio Niikawa**[13], **Jay Shendure**[3], and **Michael J. Bamshad**[1,2,3]

[1] Department of Pediatrics, University of Washington, Seattle, Washington, USA [2] Seattle Children's Hospital, Seattle, Washington, USA [3] Department of Genome Sciences, University of Washington, Seattle, Washington, USA [4] Department of Pediatrics, The Children's Hospital of Philadelphia, The University of Pennsylvania School of Medicine, Philadelphia, Pennsylvania, USA [5] Department of Human Genetics, Nagasaki University Graduate School of Biomedical Sciences, Nagasaki, Japan [6] Department of Human Genetics, Yokohama City University Graduate School of Medicine, Yokohama, Japan [7] Department of Pediatrics, Tenshi Hospital, Sapporo, Japan [8] Department of Medical Genetics, University of the Ryukyus, Okinawa, Japan [9] Department of Pediatrics, Dokkyo Medical University, Koshigaya Hospital, Saitama, Japan [10] Division of Medical Genetics, Saitama Children's Medical Center, Saitama, Japan [11] Division of Clinical Genetics, Kanagawa Children's Medical Center, Yokohama, Japan [12] Department of Pediatrics, Chang Gung Children's Hospital, Taoyuan, Taiwan, Republic of China [13] Research Institute of Personalized Health Sciences, Health Sciences University of Hokkaido, Hokkaido, Japan [14] National Laboratory of Medical Genetics, Xiangya Hospital, Central South University, Republic of China [15] Department of Pediatrics, Sapporo City General Hospital, Sapporo, Japan [16] University of Nevada School of Medicine, Las Vegas, Nevada, USA [17] Department of Genetic Medicine, Manchester Academic Health Sciences Centre, University of Manchester, England [18] Department of Pediatrics, University of Colorado, Denver, Colorado, USA

Abstract

Kabuki syndrome is a rare, multiple malformation disorder characterized by a distinctive facial appearance, cardiac anomalies, skeletal abnormalities, and mild to moderate intellectual disability. Simplex cases make up the vast majority of the reported cases with Kabuki syndrome, but parent-to-child transmission in more than a half-dozen instances indicates that it is an autosomal dominant disorder. We recently reported that Kabuki syndrome is caused by mutations in *MLL2*, a gene that encodes a Trithorax-group histone methyltransferase, a protein important in the epigenetic control of active chromatin states. Here, we report on the screening of 110 families with Kabuki syndrome. *MLL2* mutations were found in 81/110 (74%) of families. In simplex cases for which DNA was available from both parents, 25 mutations were confirmed to be *de novo*, while a transmitted *MLL2* mutation was found in two of three familial cases. The majority of variants found to cause Kabuki syndrome were novel nonsense or frameshift mutations that are predicted

Corresponding author: Mike Bamshad, MD, Department of Pediatrics, University of Washington School of Medicine, Box 356320, 1959 NE Pacific Street, Seattle, WA 98195, mbamshad@u.washington.edu, Phone: (206) 221-4131, Fax: (206) 221-3795.
*These authors contributed equally to this work.

to result in haploinsufficiency. The clinical characteristics of *MLL2* mutation-positive cases did not differ significantly from *MLL2* mutation-negative cases with the exception that renal anomalies were more common in *MLL2* mutation-positive cases. These results are important for understanding the phenotypic consequences of *MLL2* mutations for individuals and their families as well as for providing a basis for the identification of additional genes for Kabuki syndrome.

Keywords

Kabuki syndrome; *MLL2*; *ALR*; Trithorax group histone methyltransferase

INTRODUCTION

Kabuki syndrome (OMIM#147920) is a rare, multiple malformation disorder characterized by a distinctive facial appearance, cardiac anomalies, skeletal abnormalities, and mild to moderate intellectual disability. It was originally described by Niikawa et al. [1981] and Kuroki et al. [1981] in 1981, and to date, about 400 cases have been reported worldwide [Adam and Hudgins, 2005; Niikawa et al., 1988; White et al., 2004]. The spectrum of abnormalities found in individuals with Kabuki syndrome is diverse, yet virtually all affected persons are reported to have similar facial features consisting of elongated palpebral fissures, eversion of the lateral third of the lower eyelids, and broad, arched eyebrows with lateral sparseness. Additionally, affected individuals commonly have severe feeding problems, failure to thrive in infancy and height around or below the 3rd centile for age in about half of cases.

We recently reported that a majority of cases of Kabuki syndrome are caused by mutations in *mixed lineage leukemia 2* (*MLL2*; OMIM#602113), also known as either *MLL4* or *ALR* [Ng et al., 2010]. *MLL2* encodes a SET-domain-containing histone methyltransferase important in the epigenetic control of active chromatin states [FitzGerald and Diaz, 1999]. Exome sequencing revealed that nine of ten individuals had novel variants in *MLL2* that were predicted to be deleterious. A single individual had no mutation in the protein-coding exons of *MLL2*, though in retrospect, his phenotypic features are somewhat atypical of Kabuki syndrome. In a larger validation cohort screened by Sanger sequencing, we found *MLL2* mutations in approximately two-thirds of 43 Kabuki cases, suggesting that Kabuki syndrome is genetically heterogeneous.

Herein we report on the results of screening *MLL2* for mutations in 110 families with one or more individuals affected with Kabuki syndrome in order to: (1) characterize the spectrum of *MLL2* mutations that cause Kabuki syndrome; (2) determine whether *MLL2* genotype is predictive of phenotype; (3) assess whether the clinical characteristics of *MLL2* mutation-positive cases differ from *MLL2* mutation-negative cases; and (4) delineate the subset of Kabuki cases that are *MLL2* mutation-negative for further gene discovery studies.

MATERIALS AND METHODS

Subjects

Referral for inclusion into the study required a diagnosis of Kabuki syndrome made by a clinical geneticist. From these cases, phenotypic data were collected by review of medical records, phone interviews, and photographs. These data were summarized by each collaborating clinician and forwarded for review to two of the authors (MB and MH). These data were collected from five different clinical genetics centers in three different countries and over a protracted period of time and forwarded for review to two of the authors (MB and MH). Data on certain phenotypic characteristics including stature, feeding difficulties, and

failure to thrive was not uniformly collected or standardized. Therefore, we decided to be conservative in our analysis and use only phenotypic traits that could be represented by discrete variables (i.e., presence or absence) and for which data were available from at least 70% of cases. In addition, these clinical summaries were de-identified and therefore facial photographs were unavailable from most cases studied. Written consent was obtained for all participants who provided identifiable samples. The Institutional Review Boards of Seattle Children's Hospital and the University of Washington approved all studies. A summary of the clinical characteristics of 53 of these individuals diagnosed with Kabuki syndrome has been reported previously [Ng et al., 2010].

Mutation analysis

Genomic DNA was extracted using standard protocols. Each of the 54 exons of *MLL2* was amplified using Taq DNA polymerase (Invitrogen, Carlsbad, CA) following manufacturer's recommendations and using primers previously reported [Ng et al. 2010]. PCR products were purified by treatment with exonuclease I (New England Biolabs, Inc., Beverly, MA) and shrimp alkaline phosphatase (USB Corp., Cleveland, OH), and products were sequenced using the dideoxy terminator method on an automatic sequencer (ABI 3130xl). The electropherograms of both forward and reverse strands were manually reviewed using CodonCode Aligner (Dedham, MA). Primer sequences and conditions are listed in Supplementary Table I.

For *MLL2* mutation-negative samples, DNA was hybridized to commercially available whole-genome tiling arrays consisting of one million oligonucleotide probes with an average spacing of 2.6 kb throughout the genome (SurePrint G3 Human CGH Microarray 1×1M, Agilent Technologies, Santa Clara, CA). Twenty-one probes on this array covered *MLL2* specifically. Data were analyzed using Genomics Workbench software according to manufacturer's instructions.

RESULTS

All 54 protein-coding exons and intron-exon boundaries of *MLL2* were screened by Sanger sequencing in a cohort of 110 kindreds with Kabuki syndrome. This cohort included 107 simplex cases (including a pair of monozygotic twins) and three familial (i.e., parent-offspring) cases putatively diagnosed with Kabuki syndrome. Seventy novel *MLL2* variants that were inferred to be disease-causing were identified in 81/110 (74%) kindreds (Fig 1 and Supplementary Table II online). These eighty-one mutations included 37 nonsense mutations (32 different sites and five sites with recurrent mutations), three in-frame deletions or duplications (2 different sites and 1 site with a recurrent mutation), 22 frameshifts (22 different sites), 16 missense mutations (11 different sites and four sites with recurrent mutations) and 3 splice consensus site (or intron-exon boundary) mutations. None of these variants were found in dbSNP (build 132), the 1000 Genomes Project pilot data, 190 chromosomes from individuals matched for geographical ancestry. In total, pathogenic variants were found at seventy sites. Additionally, there were ten sites at which recurrent mutations were observed.

For 25 simplex cases in which we identified *MLL2* mutations, DNA was available from both unaffected parents, and in each case the mutation was confirmed to have arisen *de novo* (Supplementary Table II online). These included 14 nonsense, five frameshift, three missense, two splice site mutations and one deletion. *De novo* events were confirmed at six of the 10 sites where recurrent mutations were noted. In addition to the 81 kindreds in which we identified causal *MLL2* mutations, we found two *MLL2* variants in each of three simplex cases. In each case, neither *MLL2* mutation could unambiguously be defined as disease-causing (Supplementary Table II online). In one case, we found both a 21 bp in-frame

insertion in exon 39 and a 1 bp insertion in exon 46 predicted to cause a frameshift. However, the unaffected mother also carried the 21 bp insertion suggesting that this is a rare polymorphism, and that the 1 bp deletion is the pathogenic mutation responsible for Kabuki syndrome.

Apparent disease-causing variants were discovered in nearly half (i.e., 22/54) of all protein-coding exons of *MLL2* and in virtually every region known to encode a functional domain (Fig 1). However, the distribution of variants appeared non-random as 13 and 12 novel variants were identified in exons 48 and 39, respectively. These sites accounted for 25, or more than one-third, of all the novel *MLL2* variants and 31/81 mutations that cause Kabuki syndrome in our cohort. Eleven of the 12 pathogenic variants in exon 39 were nonsense mutations and occurred in regions that encode long polyglutamine tracts.

Four of the families studied herein had two individuals affected with Kabuki syndrome. A pair of monozygous twins with a c.15195G>A mutation were concordant for mild developmental delay, congenital heart disease, preauricular pits and palatal abnormalities, but discordant for hearing loss, and a central nervous system malformation. Concordance for mild developmental delay between an affected parent and child was observed in two families with *MLL2* mutations, one with a nonsense mutation, c.13579A>T, p.K4527X, and the other with a missense mutation, c.16391C>T, p.T5464M that was also found in a simplex case. No *MLL2* mutation was found in the remaining affected parent and child pair.

To examine the relationship between genotype and phenotype, we first compared the frequency of developmental delay, congenital heart disease, cleft lip and/or palate, and structural renal defects between *MLL2* mutation-positive vs. *MLL2* mutation-negative cases. No significant difference was observed between groups for three of these four phenotypes (Table I, a). However, renal anomalies were observed in 47% (31/66 cases) of *MLL2* mutation-positive cases compared to 14% (2/14 cases) of *MLL2* mutation-negative cases and this difference was statistically significant (χ=5.1, df=1, p=0.024). In 35 cases in two clinical cohorts for whom more complete phenotypic data were available, short stature was observed in 54% (14/26) of *MLL2* mutation-positive cases compared to 33% (3/19 cases) of *MLL2* mutation-negative cases. We also divided the *MLL2* mutation-positive cases into those with nonsense and frameshift mutations and those with missense mutations and compared the frequency of developmental delay, congenital heart disease, cleft lip and/or palate, and structural renal defects between groups. No significant differences were observed between groups (Table I, b).

In 26 independent cases of Kabuki syndrome, including one parent-offspring pair, no *MLL2* mutation was identified. Both persons in the mother-child pair had facial characteristics consistent with Kabuki syndrome (Fig 2), mild developmental delay, and no major malformations. The mother is of Cambodian ancestry and her daughter is of Cambodian and European American ancestry. In general, most of the *MLL2* mutation-negative Kabuki cases had facial characteristics (Fig 3) similar to those of the *MLL2* mutation-positive Kabuki cases, and a similar pattern of major malformations (Table I) with the exception of fewer renal abnormalities.

We screened the *MLL2* mutation-negative cases by aCGH for large deletions or duplications that encompassed *MLL2*. Abnormalities were found in four cases. In one case, a 1.87 kb deletion of chromosome 5 (hg18, chr5:175,493,803-177,361,744) that included *NSD1* and had breakpoints in flanking segmental duplications identical to the microdeletion commonly found in Sotos syndrome, was found. This suggests that this individual has Sotos syndrome, not Kabuki syndrome [Kurotaki et al., 2002]. A second case had a novel 977-kb deletion of chromosome 19q13 (hg18, chr19:61,365,420–62,342,064) encompassing 20 genes. The

majority of genes within the deleted region are zinc finger genes, some of which are known to be imprinted in both human and mouse. A third case had a complex translocation t(8;18)(q22;q21). Finally, a fourth case was found to have extra material for the entire chromosome 12. Average log2 ratio across chromosome 12 was 0.49, most likely representing mosaic aneuploidy of chromosome 12. No aCGH abnormalities were observed in 21 cases and aCGH failed for one case.

DISCUSSION

We have expanded the spectrum of mutations in *MLL2* that cause Kabuki syndrome and explored the relationship between *MLL2* genotype and some of the major, objective phenotypic characteristics of Kabuki syndrome. The majority of variants found to cause Kabuki syndrome are either novel nonsense or frameshift mutations, and appear to arise *de novo*. While mutations that cause Kabuki syndrome are found throughout the *MLL2* gene, there appear to be at least two exons (39 and 48) in which mutations are identified with a considerably higher frequency. Mutations in these three exons account for nearly half of all mutations found in *MLL2*, while the length of these exons represents ~35% of the *MLL2* open reading frame (ORF). Furthermore, exon 48, the exon in which mutations are most common, comprises only ~7% of the *MLL2* ORF. Exon 39 contains several regions that encode long polyglutamine tracts suggesting the presence of a mutational hotspot, although no such explanation is obvious for exon 48. A stepwise approach in which these regions are the first screened might be a reasonable approach to diagnostic testing. However, capture of all introns, exons, and nearby *MLL2* regulatory regions followed by next-generation sequencing would be more comprehensive and likely to be less costly over the long term.

Comparison of four of the objective clinical characteristics of *MLL2* mutation-negative versus *MLL2* mutation-positive cases allowed us to explore both the relationship between *MLL2* genotype and Kabuki phenotype and the phenotype of *MLL2* mutation-negative cases. Overall, the clinical characteristics of *MLL2* mutation-positive cases did not differ significantly from *MLL2* mutation-negative cases with the exception that renal anomalies were more common in *MLL2* mutation-positive cases. Similarly, we observed no significant phenotypic—including the severity of developmental delay—differences between individuals grouped by mutation type. However, the phenotypic data available to us for analysis was limited and, for many cases, we lacked specific information about each malformation present. Furthermore, the most typical phenotypic characteristic, the distinctive facial appearance, was not compared in detail between cases although it would be of interest to study facial images 'blinded' to mutation status to investigate its power to predict genotype. Analysis of genotype-phenotype relationships using both a larger set of Kabuki cases, and with access to more comprehensive phenotypic information would be valuable.

No *MLL2* mutation could be identified in 26 of the cases referred to us with a diagnosis of Kabuki syndrome. In three of these cases, aCGH identified structural variants that could be of clinical significance although additional investigation is required. A fourth case had the classical deletion observed in individuals with Sotos syndrome, and in retrospect it appears that this case was included in the cohort erroneously. The 22 remaining cases, including one parent-offspring pair, represent individuals with fairly classic phenotypic features of Kabuki syndrome without a *MLL2* mutation. This observation suggests that Kabuki syndrome is genetically heterogeneous. To this end, in these 22 cases, we sequenced the protein-coding exons of *UTX*, a gene that encodes a protein that directly interacts with *MLL2* but no pathogenic changes were found (data not shown). Exome sequencing of a subset of these *MLL2* mutation-negative cases to identify other candidate genes for Kabuki syndrome is underway.

Whether Kabuki syndrome is the most appropriate diagnosis for the *MLL2* mutation-negative cases is unclear. Some of the *MLL2* mutation-negative cases appear to have a facial phenotype that differs somewhat from that of the *MLL2* mutation-positive cases. Whether these *MLL2* mutation-negative cases diagnosed by expert clinicians should be considered Kabuki syndrome, a variant thereof, or a separate disorder remains to be determined. Our opinion is that there is simply not yet enough information to make an informed decision about this issue.

Most of the mutations in *MLL2* are predicted to result in haploinsufficiency. However, it is unclear by what mechanism(s) haploinsufficiency of *MLL2* could cause Kabuki syndrome. *MLL2* encodes a histone 3 lysine 4 (H3K4) methyltransferase, one of at least 10 proteins (genes for which have not to our knowledge yet been screened in Kaubki cases in which *MLL2* mutations were not found) that have been identified to specifically modify the lysine residue at the fourth amino acid position of the histone H3 protein [Kouzarides, 2007]. MLL2 has a SET domain near its C-terminus that is shared by yeast Set1, *Drosophila* Trithorax (TRX) and human MLL1 [FitzGerald and Diaz, 1999]. MLL2 appears to regulate gene transcription and chromatin structure in early development [Prasad et al., 1997]. In mice, loss of *MLL2* results in embryonic lethality before E10.5, and while *Mll2*$^{+/-}$ mice are viable, they are smaller than wild type (Kai Ge, personal communication).

Kabuki syndrome is the most common of a small, but growing group of multiple malformation syndromes accompanied by developmental delay that are caused by mutations in genes that encode proteins involved in histone methylation [De Sario, 2009]. The most notable of these is CHARGE syndrome, which is one of the syndromes often considered in the differential diagnosis of children ultimately diagnosed with Kabuki syndrome. CHARGE syndrome is caused by mutations in *CHD7*, which encodes a chromodomain protein that recognizes the trimethylated H3K4 side chain [Vissers et al., 2004]. Other disorders caused by defects of histone methylation status include several intellectual disability syndromes, some of which are also characterized by malformations (e.g., cleft lip/palate) that overlap with those found in individuals with Kabuki syndrome.

Kabuki syndrome is one of the most common causes of heritable developmental delay. Discovery that mutations in *MLL2* are the most common cause of Kabuki syndrome highlights the role that disrupted regulation of histone methylation plays as a cause of human birth defects. Characterizing the spectrum of mutations in *MLL2* is a small but important first step toward understanding the mechanism(s) that underlies Kabuki syndrome.

Supplementary Material

Refer to Web version on PubMed Central for supplementary material.

Acknowledgments

We thank the families for their participation and the Kabuki Syndrome Network for their support. Our work was supported in part by grants from the National Institutes of Health/National Heart Lung and Blood Institute (5R01HL094976 to D.A.N. and J.S.), the National Institutes of Health/National Human Genome Research Institute (5R21HG004749 to J.S., 1RC2HG005608 to M.J.B., D.A.N., and J.S.; and 5RO1HG004316 to H.K.T.), National Institute of Heath/National Institute of Environmental Health Sciences (HHSN273200800010C to D.N. and M.R.), National Institute of Neurological Disorders and Stroke (RO1NS35102 to C.S.M.) NIHR Manchester Biomedical Research Centre (D. D.), Ministry of Health, Labour and Welfare (K.Y., N.M., T.O., and N.N.), Ministry of Health, Labour and Welfare of Japan (N.M), Japan Science and Technology Agency (N.M.), Society for the Promotion of Science (N.M.), the Life Sciences Discovery Fund (2065508 and 0905001), the Washington Research Foundation, and the National Institutes of Health/National Institute of Child Health and Human Development (1R01HD048895 to M.J.B. and 5K23HD057331 to A.E.B.). S.B.N. is supported by the Agency for Science, Technology and Research, Singapore. A.W.B. is supported by a training fellowship from the National Institutes of Health/National Human Genome Research Institute (T32HG00035).

References

Adam MP, Hudgins L. Kabuki syndrome: a review. Clin Genet. 2005; 67(3):209–219. [PubMed: 15691356]

De Sario A. Clinical and molecular overview of inherited disorders resulting from epigenomic dysregulation. Eur J Med Genet. 2009; 52(6):363–372. [PubMed: 19632366]

FitzGerald KT, Diaz MO. MLL2: A new mammalian member of the trx/MLL family of genes. Genomics. 1999; 59(2):187–192. [PubMed: 10409430]

Kouzarides T. Chromatin modifications and their function. Cell. 2007; 128(4):693–705. [PubMed: 17320507]

Kuroki Y, Suzuki Y, Chyo H, Hata A, Matsui I. A new malformation syndrome of long palpebral fissures, large ears, depressed nasal tip, and skeletal anomalies associated with postnatal dwarfism and mental retardation. J Pediatr. 1981; 99(4):570–573. [PubMed: 7277097]

Kurotaki N, Imaizumi K, Harada N, Masuno M, Kondoh T, Nagai T, Ohashi H, Naritomi K, Tsukahara M, Makita Y, Sugimoto T, Sonoda T, Hasegawa T, Chinen Y, Tomita Ha HA, Kinoshita A, Mizuguchi T, Yoshiura Ki K, Ohta T, Kishino T, Fukushima Y, Niikawa N, Matsumoto N. Haploinsufficiency of NSD1 causes Sotos syndrome. Nat Genet. 2002; 30(4):365–366. [PubMed: 11896389]

Ng SB, Bigham AW, Buckingham KJ, Hannibal MC, McMillin MJ, Gildersleeve HI, Beck AE, Tabor HK, Cooper GM, Mefford HC, Lee C, Turner EH, Smith JD, Rieder MJ, Yoshiura K, Matsumoto N, Ohta T, Niikawa N, Nickerson DA, Bamshad MJ, Shendure J. Exome sequencing identifies MLL2 mutations as a cause of Kabuki syndrome. Nat Genet. 2010; 42(9):790–793. [PubMed: 20711175]

Niikawa N, Kuroki Y, Kajii T, Matsuura N, Ishikiriyama S, Tonoki H, Ishikawa N, Yamada Y, Fujita M, Umemoto H, et al. Kabuki make-up (Niikawa-Kuroki) syndrome: a study of 62 patients. Am J Med Genet. 1988; 31(3):565–589. [PubMed: 3067577]

Niikawa N, Matsuura N, Fukushima Y, Ohsawa T, Kajii T. Kabuki make-up syndrome: a syndrome of mental retardation, unusual facies, large and protruding ears, and postnatal growth deficiency. J Pediatr. 1981; 99(4):565–569. [PubMed: 7277096]

Prasad R, Zhadanov AB, Sedkov Y, Bullrich F, Druck T, Rallapalli R, Yano T, Alder H, Croce CM, Huebner K, Mazo A, Canaani E. Structure and expression pattern of human ALR, a novel gene with strong homology to ALL-1 involved in acute leukemia and to Drosophila trithorax. Oncogene. 1997; 15(5):549–560. [PubMed: 9247308]

Vissers LE, van Ravenswaaij CM, Admiraal R, Hurst JA, de Vries BB, Janssen IM, van der Vliet WA, Huys EH, de Jong PJ, Hamel BC, Schoenmakers EF, Brunner HG, Veltman JA, van Kessel AG. Mutations in a new member of the chromodomain gene family cause CHARGE syndrome. Nat Genet. 2004; 36(9):955–957. [PubMed: 15300250]

White SM, Thompson EM, Kidd A, Savarirayan R, Turner A, Amor D, Delatycki MB, Fahey M, Baxendale A, White S, Haan E, Gibson K, Halliday JL, Bankier A. Growth, behavior, and clinical findings in 27 patients with Kabuki (Niikawa-Kuroki) syndrome. Am J Med Genet A. 2004; 127A(2):118–127. [PubMed: 15108197]

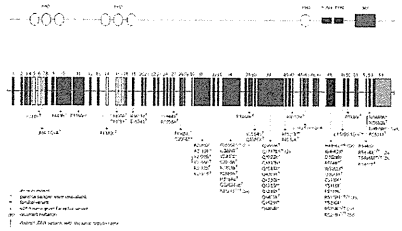

Figure 1. Genomic structure and allelic spectrum of *MLL2* mutations that cause Kabuki syndrome

MLL2 is composed of 54 exons that include untranslated regions (orange) and protein coding sequence (blue) including 7 PHD fingers (yellow), FYRN (green), FYRC (green), and a SET domain (red). Arrows indicate the locations of 81 mutations affecting 70 sites found in 110 families with Kabuki syndrome including: 37 nonsense, 22 frameshifts, 16 missense, 3 in-frame deletions/duplications, and 3 splice-site mutations. Asterisks indicate mutations that were confirmed to be *de novo* and crosses indicate cases for which parental DNA was unavailable.

Figure 2.
Facial photographs of mother and daughter with Kabuki syndrome in whom no causative mutation in *MLL2* was identified. Both have mild developmental delay and no known major malformations.

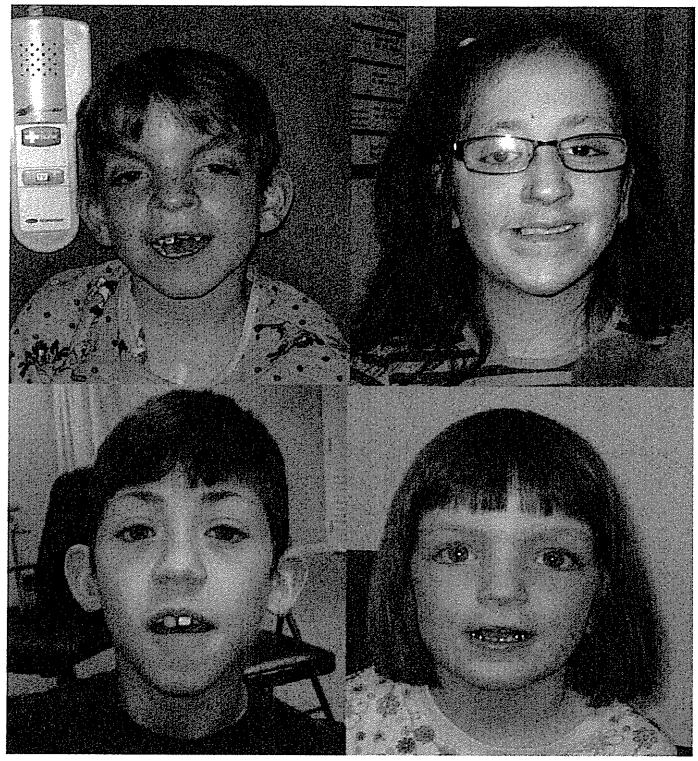

Figure 3.
Facial photographs of four children diagnosed with Kabuki syndrome in whom no causative mutation in *MLL2* was found.

Table I

Phenotypic traits grouped by *MLL2* mutation status (a) and type (b)

Trait	***MLL2*+**	***MLL2*−**
Intellectual Disability	74/74 (100%)	19/20 (95%)
Mild	51/74 (69%)	10/20 (50%)
Moderate	18/74 (24%)	4/20 (20%)
Severe	4/74 (5%)	3/20 (15%)
Cleft palate, CL/CP	29/72 (40%)	8/18 (44%)
Congenital heart defect	36/71 (51%)	8/19 (42%)
Renal abnormality	31/66 (47%)	2/14 (14%)
Trait	**Truncating (N=59)**	**Missense (N=16)**
Intellectual disability	54/54 (100%)	15/15 (100%)
Mild	36/54 (67%)	11/15 (73 %)
Moderate	13/54 (24%)	4/15 (27%)
Severe	5/54 (9%)	0/15
Cleft palate, CL/CP	23/54 (43%)	3/14 (21%)
Congenital heart defect	30/54 (55%)	4/13 (30%)
Renal anomaly	9/44 (20%)	2/12 (17%)

CLINICAL GENETICS An International Journal of Genetics, Molecular and Personalized Medicine

Clin Genet 2011: 80: 161–166
Printed in Singapore. All rights reserved

CLINICAL GENETICS
doi: 10.1111/j.1399-0004.2011.01721.x

Short Report

Exome sequencing of two patients in a family with atypical X-linked leukodystrophy

Tsurusaki Y, Okamoto N, Suzuki Y, Doi H, Saitsu H, Miyake N, Matsumoto N. Exome sequencing of two patients in a family with atypical X-linked leukodystrophy.
Clin Genet 2011: 80: 161–166. © John Wiley & Sons A/S, 2011

We encountered a family with two boys similarly showing brain atrophy with reduced white matter, hypoplasia of the brain stem and corpus callosum, spastic paralysis, and severe growth and mental retardation without speaking a word. The phenotype of these patients was not compatible with any known type of syndromic leukodystrophy. Presuming an X-linked disorder, we performed next-generation sequencing (NGS) of the transcripts of the entire X chromosome. A single lane of exome NGS in each patient was sufficient. Six potential mutations were found in both affected boys. Two missense mutations, including c.92T>C (p.V31A) in *L1CAM*, were potentially pathogenic, but this remained inconclusive. The other four could be excluded. Because the patients did not show adducted thumbs or hydrocephalus, the *L1CAM* change in this family can be interpreted as different scenarios. Personal genome analysis using NGS is certainly powerful, but interpretation of the data can be a substantial challenge requiring a lot of tasks.

Conflict of interest

None of the authors have any conflicts of interest to disclose.

Y Tsurusaki[a], N Okamoto[b], Y Suzuki[c], H Doi[a], H Saitsu[a], N Miyake[a] and N Matsumoto[a]

[a]Department of Human Genetics, Yokohama City University Graduate School of Medicine, Kanazawa-ku, Yokohama, Japan, and [b]Department of Medical Genetics, and [c]Department of Pediatric Neurology, Osaka Medical Center and Research Institute for Maternal and Child Health, Murodo-cho, Izumi, Japan

Key words: atypical phenotype – exome sequencing – *L1CAM* – X-linked leukodystrophy

Corresponding author: Naomichi Matsumoto, Department of Human Genetics, Yokohama City University Graduate School of Medicine, 3-9 Fukuura, Kanazawa-ku, Yokohama 236-0004, Japan.
Tel.: +81-45-787-2606;
fax: +81-45-786-5219;
e-mail: naomat@yokohama-cu.ac.jp

Received 4 May 2011, revised and accepted for publication 31 May 2011

Focused/selected gene and genomic characterization has usually been carried out in clinically homogeneous groups of multiple affected samples to make identification of genetic abnormalities more efficient. Microarrays and next-generation sequencing (NGS) have provided new avenues for human genetic research (1–6). Using such new technologies, researchers are able to analyze small numbers of patients on a genome-wide scale. Even very rare cases (such as when only a few compatible patients are available or atypical patients showing no similar phenotypes) can be realistic targets of genetic research, as the new technologies can identify aberrations in a single gene from within virtually the whole genome; this could not be achieved with conventional techniques.

We encountered a family with two affected males showing atypical leukodystrophy. The phenotype of these patients did not match any known type of syndromic leukodystrophy. Because we presumed that abnormality of an X-linked gene caused the atypical leukodystrophy in this family, we performed exome sequencing of most of the X-chromosome transcripts and identified an unexpected gene mutation in these patients.

Materials and methods

A family with atypical X-linked leukodystrophy

Two brothers, II-1 currently aged 19 years and II-2 currently aged 17 years, who have unrelated healthy parents, presented with similar clinical

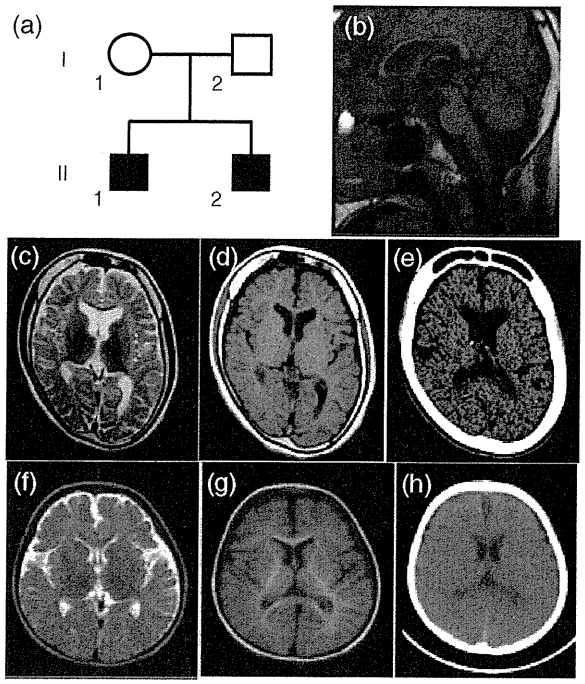

Fig. 1. Clinical features of the family. Familial pedigree (**a**). Brain magnetic resonance imaging (MRI) (**b**: T1-weighted image, **c**: T2-weighted image, **d**: T1-weighted image) of individual II-1 at 16 years old showing hypoplasia of the white matter, the brain stem and the corpus callosum. Brain computed tomographic (CT) images of individual II-1 at 19 years old (**e**) indicating a thick calvarium with enlarged frontal sinus as well as calcification of the choroid plexus in the atrophic brain. Brain MRI (**f**: T2-weighted image, **g**: T1-weighted image) of individual II-2 at 2 years old, also displaying hypoplasia of the white matter. Brain CT image of individual II-2 at 5 years old (**h**), also showing a thick calvarium.

features. Their mother did not show any neurological abnormalities (Fig. 1a).

Patient II-1

Patient II-1's birth weight was 2840 g at 40 weeks of gestational age. He had congenital nystagmus. He sat unsupported at 7 months old but after this his developmental milestones were delayed. He could creep at 18 months old. Spastic paralysis, especially in the lower extremities, became apparent. He was unable to stand unsupported. His mental development was severely delayed, and he needed special education from elementary school. He had suffered generalized epileptic seizures since he was 10 years old. He was confined to a wheelchair. He had severe mental retardation without speaking a word. His developmental quotient (DQ) at 9 years old was 19 by the Japanese standard method. Severe growth retardation [143 cm (<3%), 24 kg (<3%), occipitofrontal head circumference 49 cm (<3%) at 19 years] was also noted. He did not have dysmorphic features. Blood analysis revealed microcytic anemia [hemoglobin (Hb) 13.4 g/dl, mean corpuscular volume (MCV) (of red blood cell) 70.4 fl (normal: 89–99 fl), mean corpuscular hemoglobin (MCH) (of red blood cell) 23.1 pg (normal: 29–35 pg)] without any evidence of hemolysis or iron deficiency. Hormonal examination indicated that the levels of luteinizing hormone, follicle-stimulating hormone, and thyroid-stimulating hormone were all low [0.9 mIU/ml (normal: 1.2–8.0 mIU/ml), 2.5 mIU/ml (normal: 2.3–15.1 mIU/ml), <0.01 μIU/ml (normal: 0.5–5.0 μIU/ml), respectively]. He showed delayed puberty with small testes. Pubic hair only appeared at 17 years old. His bone age at 18 years old was 12.6 years (67%). Brain magnetic resonance imaging (MRI) at 16 years old revealed brain atrophy associated with reduced white matter and hypoplasia of the brain stem and the corpus callosum (Fig. 1b–d). No hydrocephalus or adducted thumb was observed. Brain computed tomography (CT) at 19 years old showed a thick calvarium with enlarged frontal sinus as well as calcification of the cerebellar tentorium and the choroid plexus (Fig. 1e).

Patient II-2

Patient II-2's birth weight was 2910 g at 37 weeks of gestational age. Developmental delay was apparent since he was 10 months old. Spastic paralysis (especially in the lower extremities), confinement to a wheelchair, severe mental retardation without speaking a word (DQ = 5 at 17 years old), and severe growth retardation [130 cm (<3%) and 27 kg (<3%) at 17 years] were phenotypes shared with his brother (II-1). Blood analysis revealed microcytic anemia (Hb 12.0 g/dl, MCV 61.1 fl, MCH 19.0 pg) without any evidence of hemolysis or iron deficiency. Hormonal examination indicated that the levels of luteinizing hormone, follicle-stimulating hormone, and thyroid-stimulating hormone were relatively low (1.9 mIU/ml, 4.2 mIU/ml, <0.23 μIU/ml, respectively). He also showed delayed puberty with small testes. Pubic hair appeared only at 17 years old. His bone age at 17 years old was 11 years (65%). Brain MRI at 2 years old revealed brain atrophy associated with reduced white matter and hypoplasia of the brain stem and corpus callosum (Fig. 1f,g). Brain CT at 5 years old showed a thick calvarium (Fig. 1h). No hydrocephalus or adducted thumb was observed. Most of the clinical features were similar to those of his brother except for the absence of nystagmus in patient II-2.

Genome-wide SNP genotyping

Genome-wide single-nucleotide polymorphism (SNP) genotyping was performed on individuals I-2, II-1, and II-2 using a GeneChip™ Human Mapping 10K Array Xba 142 2.0 (Affymetrix, Inc., Santa Clara, CA), according to the manufacturer's protocols. Mendelian error in the pedigree to exclude conflicted SNPs was checked using GCOS 1.2 (GeneChip Operating Software; Affymetrix) and batch analysis in GTYPE 4.0 (GeneChip Genotyping Analysis Software; Affymetrix), with the default setting for the mapping algorithm. The linked region, with SNP genotypes shared between individuals II-1 and II-2, was checked manually.

Genomic partitioning, short-read sequencing, and sequence alignment

Three micrograms of genomic DNA from the affected brothers (II-1 and II-2) was processed using a SureSelect X Chromosome test kit (1582 transcripts covering 3053 kb) (Agilent Technologies, Santa Clara, CA), according to the manufacturer's instructions. Captured DNAs were analyzed using an Illumina GAIIx (Illumina, Inc., San Diego, CA). We used only one of the eight lanes in the flow cell (Illumina) for paired-end, 76-bp reads per sample. Image analysis and base-calling were performed using sequence control software (SCS) real-time analysis and off-line BASECALLER software v1.8.0 (Illumina). Reads were aligned to the human reference genome (UCSC hg19, NCBI build 37.1) using the ELANDv2 algorithm in CASAVA_v1.7.0 (Illumina). The ELANDv2 algorithm can align 100-bp reads to a reference sequence and split the reads into multiple seeds.

Mapping strategy and variant annotation

Approximately 57.5 million reads from individual II-1 and 71.1 million reads from individual II-2 that passed the quality control (Path Filter) were mapped to the human reference genome using mapping and assembly with quality (MAQ) (7) (Fig. 2). MAQ was able to align 51 720 952 and 65 990 660 reads to the whole genome for individuals II-1 and II-2, respectively; these were then statistically analyzed for coverage using a script created by BITS Co., Ltd. (Tokyo, Japan). SNPs and insertions/deletions were extracted from the alignment data using an original script created by BITS Co., Ltd., along with information on the registered SNPs (dbSNP 131). A consensus quality score of 40 or more was used for the SNP analysis in MAQ. SNPs in MAQ-passed reads were annotated using the SeattleSeq website (http://gvs.gs.washington.edu/SeattleSeqAnnotation/). Variants found by each informatics method were selected in terms of location on chromosome X, unregistered variants (excluding registered SNPs), variants in known genes, variants in coding regions, variants excluding synonymous changes, and variants with an allele frequency of at least 90% (assuming a homozygous mutation). NEXTGENE software v2.0 (SoftGenetics, State College, PA) was also used to analyze the reads, with a default setting. Variants found by both of the informatics methods were selected. The variants found in common between individuals II-1 and II-2 were focused on, and confirmed as true positives by Sanger sequencing of polymerase chain reaction (PCR) products amplified from patient genomic DNA, except for variants within genes at segmental duplications. The pathological significance of the variants was evaluated using four different websites: POLYPHEN (Polymorphism Phenotyping; http://genetics.bwh.harvard.edu/pph/index.html), POLYPHEN-2 (http://genetics.bwh.harvard.edu/pph2/index.shtml), SIFT (http://sift.jcvi.org/) (output values less than 0.05 are deleterious), and MUTATIONTASTER (http://neurocore.charite.de/MutationTaster/).

Capillary sequencing

Possible pathological variants were confirmed by Sanger sequencing using an ABI 3500xl or ABI3100 autosequencer (Life Technologies, Carlsbad, CA), following the manufacturer's protocol. Sequencing data were analyzed using SEQUENCHER software (Gene Codes Corporation, Ann Arbor, MI).

Expression studies

The relative mRNA levels of *TMEM187* in cDNA of various fetal and adult human tissues (Human MTC™ Panel I and Human Fetal MTC™ Panel; Clontech, Mountain View, CA) were determined by quantitative real-time reverse transcription–polymerase chain reaction (RT-PCR) using TaqMan gene expression assays (Hs01920894_s1 for *TMEM187* and Hs00357333_g1 for β-actin as a control) (Life Technologies).

Results and discussion

Our coverage analysis indicated that for individuals II-1 and II-2, 79.2% and 78.8%, respectively, of the entire X-chromosome coding sequence (CDS) were completely covered, and 88.5% and 88.5%,

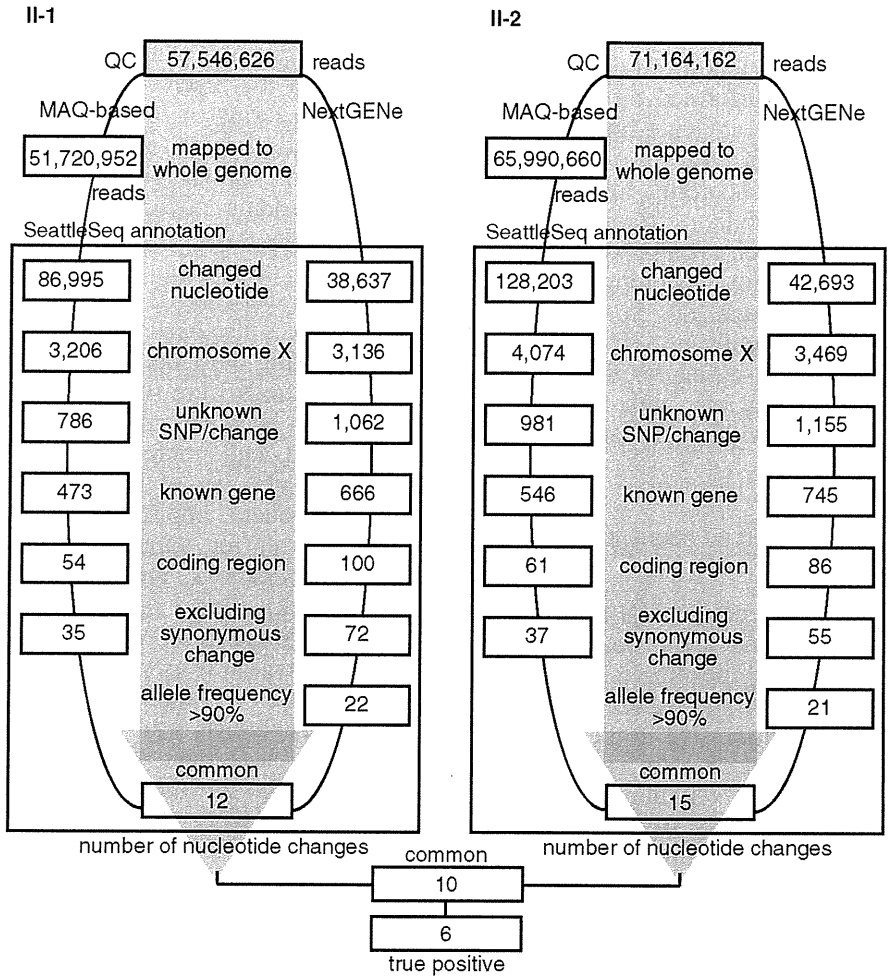

Fig. 2. Flow of informatics analysis. A MAQ-based method and NextGENe analysis were performed in individuals II-1 and II-2. The selection methods employed included variants compared with the human genome reference sequence, variants mapped to chromosome X, unknown variants [excluding registered single-nucleotide polymorphisms (SNPs)], variants in known genes, variants in coding regions, variants excluding synonymous changes, and variants common to the two informatics methods. Finally, the nucleotide changes in common between individuals II-1 and II-2 were focused on as potentially pathogenic mutations. True positive changes were confirmed by capillary sequencing of polymerase chain reaction (PCR) products amplified from genomic DNA.

respectively, of the CDS were at least 90% covered by reads. Using a single lane of sequencing per sample, the coverage with 20 reads or more comprised 89.6% and 89.7% of the CDS, and that with 100 reads or more comprised 87.6% and 89.7% of the CDS in individuals II-1 and II-2, respectively. SNP genotyping indicated that the region from rs727240 to rs721003 (UCSC genome browser hg19 assembly, chromosome X coordinates: 22131639–54454152; 32.2 Mb) was unlinked to the phenotype. Exome sequencing using two informatics methods successfully identified six potentially interesting changes as true positives in the linked region: *FAM123B* (RefSeq Gene ID NM_152424): c.85G>A (p.A29T), *FRMD7* (NM_194277): c.875T>C (p.L292P), *L1CAM* (NM_000425): c.92T>C (p.V31A), *TMEM187* (NM_003492): c.334G>A (p.A112T), *FLNA* (NM_001110556): c.1582G>A (p.V528M), and *LAGE3* (NM_006014): c.395G>A (p.R132Q).

The c.92T>C (p.V31A) variant in *L1CAM* was previously found in a patient with Hirschsprung disease, acrocallosal syndrome, and congenital hydrocephalus (8). *L1CAM* mutations cause a wide variety of clinical phenotypes: hydrocephalus due to stenosis of the aqueduct of Sylvius (MIM #307000), MASA syndrome (mental retardation, aphasia, shuffling gait, adducted thumb; MIM #303350), and X-linked agenesis of the corpus callosum (MIM #217990). Phenotypic variability, even within a family, has been noted, raising the caution that definite clinical diagnosis in single

Table 1. Characterization of nucleotide changes found by exome sequencing

	FAM123B	*FRMD7*	*L1CAM*	*TMEM187*	*FLNA*	*LAGE3*
Change	c.85G>A (p.A29T)	c.875T>C (p.L292P)	c.92T>C (p.V31A)	c.334G>A (p.A112T)	c.1582G>A (p.V528M)	c.395G>A (p.R132Q)
PolyPhen	Benign	Probably damaging	Benign	Benign	Possibly damaging	Benign
PolyPhen-2	Probably damaging	Probably damaging	Benign	Possibly damaging	Possibly damaging	Possibly damaging
SIFT	0.04	0.02	0.22	0.02	0.04	0.46
MutationTaster	Polymorphism	Disease causing	Disease causing	Polymorphism	Polymorphism	Polymorphism
Normal female	8/502[a]	2/502	2/502	1/502	15/502[a]	4/502
Normal male	1/118	0/117	0/118	0/118		1/86
Note		No nystagmus in II-2				

[a]Including one homozygous female. Underlining means that this result excludes the variant as potentially causative. Grayed shading indicates the variants that could not be excluded; between these two, the *L1CAM* variant is more likely to be causative.

cases is often impossible (9). Phenotypic features compatible with the *L1CAM* mutation in our patients include spastic paralysis, aphasia, severe mental and growth retardation, but atypical leukodystrophy and the absence of adducted thumbs were very rare or exceptional (9). A normal control study found that 2 of 251 normal females were heterozygous for this SNP, but none of 117 normal males carried the variant allele. One of the four web-based analyses of pathological significance (MutationTaster) indicated that this variant would be disease causing, while the others indicated that it would be benign (Table 1). X-linked hydrocephalus due to *L1CAM* mutations occurs in approximately 1/30 000 male births (10). Considering that the *L1CAM* mutation was found in 2/618 control alleles (0.32%), the change may be a rare polymorphism, a mutation causing lethality in the majority of affected males, or a mutation with low penetrance. Because we were unable to exclude this *L1CAM* change, its pathogenic status remains inconclusive.

We next examined c.85G>A in *FAM123B*, c.875T>C in *FRMD7*, c.1582G>A in *FLNA*, and c.395G>A in *LAGE3* in normal controls. The *FAM123B*, *FLNA*, and *LAGE3* variants were excluded as causative because a homozygous change was found in 1 of 251 female controls (*FAM123B* and *FLNA*) or a hemizygous change was found in 1 of 86 normal males (*LAGE3*). However, the thick calvarium in individuals II-1 and II-2 may be influenced by the *FAM123B* change, because it is causative for osteopathia striata with cranial sclerosis, an X-linked dominant disorder (MIM #300373) (11, 12). As the calvarium of the patients' mother having the heterozygous *FAM123B* change was not evaluated by CT, we could not confirm this possibility.

Only 2 of 251 control females carried the c.875T>C variant in *FRMD7* heterozygously, and none of 117 male controls carried this variant; thus, the pathogenicity of the *FMRD7* variant was inconclusive. Other *FRMD7* mutations cause X-linked congenital nystagmus 1 (MIM #310700) (13). However, the nystagmus found in individual II-1 was not observed in individual II-2, indicating that the variant in common between two brothers did not consistently cause nystagmus. Thus, it may not contribute to the phenotype in this family (Table 1).

We also evaluated the c.334G>A variant in *TMEM187*. Only 2 of 251 female controls carried this heterozygous change, and it was not found among 118 male controls. Two of the four programs (PolyPhen-2 and SIFT) indicated that it would be pathogenic. By Taqman assay, *TMEM187* was ubiquitously expressed in various fetal and adult tissues, including the brain (data not shown), leaving the effect of this mutation on the phenotype in these patients inconclusive (Table 1).

In conclusion, we found two possible but inconclusive variants in this family with two boys affected by atypical leukodystrophy. High-throughput technologies are clearly powerful to detect genomic changes, but evaluation of the data can be very difficult and should be performed cautiously. More knowledge of rare SNPs and mutations is absolutely necessary before any conclusions can be drawn.

Acknowledgements

We would like to thank the patients and their family members for their participation in this study. This work was supported by research grants from the Ministry of Health, Labour and Welfare

(to H. S., N. Miyake, and N. Matsumoto), the Japan Science and Technology Agency (to N. Matsumoto), a Grant-in-Aid for Scientific Research from the Japan Society for the Promotion of Science (to N. Matsumoto), and a Grant-in-Aid for Young Scientists from the Japan Society for the Promotion of Science (to H. D., N. Miyake, and H. S.).

References

1. Saitsu H, Kato M, Mizuguchi T et al. De novo mutations in the gene encoding STXBP1 (MUNC18-1) cause early infantile epileptic encephalopathy. Nat Genet 2008: 40: 782–788.
2. Check Hayden E. Genomics shifts focus to rare diseases. Nature 2009: 461: 458.
3. Biesecker LG. Exome sequencing makes medical genomics a reality. Nat Genet 2010: 42: 13–14.
4. Kuhlenbaumer G, Hullmann J, Appenzeller S. Novel genomic techniques open new avenues in the analysis of monogenic disorders. Hum Mutat 2011: 32: 144–151.
5. Miyake N, Kosho T, Mizumoto S et al. Loss-of-function mutations of CHST14 in a new type of Ehlers-Danlos syndrome. Hum Mutat 2010: 31: 966–974.
6. Ng SB, Bigham AW, Buckingham KJ et al. Exome sequencing identifies MLL2 mutations as a cause of Kabuki syndrome. Nat Genet 2010: 42: 790–793.
7. Li H, Ruan J, Durbin R. Mapping short DNA sequencing reads and calling variants using mapping quality scores. Genome Res 2008: 18: 1851–1858.
8. Nakakimura S, Sasaki F, Okada T et al. Hirschsprung's disease, acrocallosal syndrome, and congenital hydrocephalus: report of 2 patients and literature review. J Pediatr Surg 2008: 43: E13–E17.
9. Rietschel M, Friedl W, Uhlhaas S, Neugebauer M, Heimann D, Zerres K. MASA syndrome: clinical variability and linkage analysis. Am J Med Genet 1991: 41: 10–14.
10. Rosenthal A, Jouet M, Kenwrick S. Aberrant splicing of neural cell adhesion molecule L1 mRNA in a family with X-linked hydrocephalus. Nat Genet 1992: 2: 107–112.
11. Viot G, Lacombe D, David A et al. Osteopathia striata cranial sclerosis: non-random X-inactivation suggestive of X-linked dominant inheritance. Am J Med Genet 2002: 107: 1–4.
12. Jenkins ZA, van Kogelenberg M, Morgan T et al. Germline mutations in WTX cause a sclerosing skeletal dysplasia but do not predispose to tumorigenesis. Nat Genet 2009: 41: 95–100.
13. Tarpey P, Thomas S, Sarvananthan N et al. Mutations in FRMD7, a newly identified member of the FERM family, cause X-linked idiopathic congenital nystagmus. Nat Genet 2006: 38: 1242–1244.